WATER RESOURCES RESEARCH, VOL. 35, NO. 10, PAGES 2955–2964, OCTOBER 1999

The entrapment and long-term dissolution of tetrachloroethylene in fractional wettability porous media

Scott A. Bradford, Richard A. Vendlinski, and Linda M. Abriola
Department of Civil and Environmental Engineering, University of Michigan, Ann Arbor

Abstract. Theoretical and modeling studies for the prediction of nonaqueous phase liquid (NAPL) entrapment and dissolution have largely assumed that the soil is preferentially water-wet. Many natural systems, however, have both water- and NAPL-wet solids as a result of spatial and temporal variations in fluid and soil properties. This condition is referred to as fractional wettability. This work presents long-term dissolution data for tetrachloroethylene (PCE) entrapped in porous media representing a range of grain sizes, gradations, and fractional wettabilities. Entrapment data suggest that for given wettability conditions, initial residual NAPL saturations tend to increase with decreasing soil mean grain size. In addition, residual NAPL saturations in finer-textured sands were observed to reach a minimum at intermediate wetting conditions, whereas residual saturations in coarser-textured media decreased asymptotically with increasing fraction of NAPL-wet sand. In dissolution studies, an increase in the NAPL-wet fraction tended to result in decreased PCE dissolution time, characterized by a longer period of high effluent concentrations, followed by a more rapid reduction in concentration. Increases in NAPL-wet fraction, however, were also associated with higher sorptive capacities, leading to enhanced PCE concentration tailing. The influence of fractional wettability on PCE dissolution behavior was also found to depend on media grain size distribution, particularly for more water-wet soils. Experimental observations are discussed in the context of pore-scale conceptual models of entrapment.

1. Introduction

The improper storage and disposal of hazardous nonaqueous phase liquids (NAPLs) has resulted in widespread contamination of the subsurface environment [*Dragun et al*., 1984]. As a NAPL migrates within a formation, a portion is retained within the pore structure owing to capillary forces. This entrapped residual NAPL serves as a persistent source of pollution to flowing groundwater. Our ability to predict the performance of a particular remediation technology in a NAPL contaminated formation will be determined, to a large extent, by our understanding of the processes that control interphase mass transfer. Indeed, the success of conventional "pump-and-treat" groundwater remediation technologies [*Kavanaugh*, 1996] is now widely recognized to be controlled by the slow dissolution of residual NAPL to the aqueous phase.

Subsurface systems containing NAPL and water are generally assumed to be preferentially wetted by water. In water-wet systems, water occupies the smaller pores and the pore space immediately adjacent to the soil grains in the larger pores; residual NAPL is entrapped in the center of the larger pores as discontinuous spherical singlets or ganglia [*Chatzis et al*., 1983]. Entrapped NAPL ganglia may be quite complex in shape, occupying multiple pore bodies. These shapes are controlled by variations in pore structure and size, as well as by the initial NAPL release rate and saturation history [*Land*, 1968]. Studies in etched-glass micromodels that mimic the pore structure in natural media [*Wilson et al*., 1990] and observations of ganglia cast within porous media [*Mayer and Miller*, 1992; *Powers et al*., 1992] have confirmed this conceptual model.

The configuration of residual NAPL in natural subsurface systems can be more complex than that in water-wet sands and/or glass beads owing to variations in aqueous chemistry [*Demond et al*., 1994], mineralogy [*Anderson*, 1986], organic matter distributions [*Dekker and Ritsema*, 1994], surface roughness [*Morrow*, 1975], and contaminant aging [*Powers and Tamblin*, 1995]. Some porous media have both water- and NAPL-wet solid surfaces. This condition is referred to as fractional wettability. In petroleum reservoirs, fractional wettability has been recognized as a ubiquitous condition [*Brown and Fatt*, 1956; *Donaldson et al*., 1969; *Salathiel*, 1973]. In a fractional wettability medium the residual NAPL can potentially be entrapped as multipore NAPL ganglia and singlets, typical of water-wet porous media, and as NAPL films coating some of the solid surfaces.

Changes in the pore-scale configuration of residual NAPL due to wettability variations have been reported to influence the NAPL-water interfacial area [*Bradford and Leij*, 1997] and the aqueous flow field [*Wang*, 1988]. Because interphase mass transfer processes have been demonstrated to be sensitive to system hydrodynamics and interfacial area [e.g., *Powers et al*., 1994a; *Abriola and Bradford*, 1998], it is logical to anticipate that dissolution will also be influenced by wettability variations. For example, at a particular NAPL saturation the NAPL-water interfacial area will be much higher when the NAPL is distributed as a film than when it is entrapped as singlets [*Gvirtzman and Roberts*, 1991]. Consequently, enhanced dissolution would be expected in fractional wettability systems. The accessibility of the residual NAPL to the flowing aqueous phase will also be influenced by the pore-scale NAPL configuration. Ganglia en-

Paper number 1999WR900178.
0043-1397/99/1999WR900178$09.00

Table 1. Porous Medium Properties

	F20-F30	F35	F50	F70	F110	Median Grain Size d_{50}, cm	Uniformity Index U_i	OTS%*
F20-F30	100%	···	···	···	···	0.071	1.21	0, 10, 25, 50, 75
F35-F50	···	50%	50%	···	···	0.036	1.88	0, 10, 25, 50, 75, 100
F70-F110	···	···	···	50%	50%	0.015	2.25	0, 10, 25, 50, 75, 100
F35-F50-F70-F110	···	25%	25%	25%	25%	0.024	3.06	0, 10, 25, 50, 75, 100

*Mass fraction treated with octadecyltrichlorosilane.

trapped in water-wet solids are primarily found in a narrow range of larger pores. In contrast, residual NAPL films may exist within a much wider range of pore classes. Some of these pore classes, however, may be less accessible to a flowing aqueous phase.

Most previous experimental dissolution studies have been conducted in water-wet glass beads or silica sands [i.e., *Pfannkuch*, 1984; *Hunt et al*., 1988; *Geller and Hunt*, 1993; *Parker et al*., 1991; *Miller et al*., 1990; *Powers et al*., 1992; *Guarnaccia et al*., 1992; *Imhoff et al*., 1994]. Similarly, predictive approaches to describe the dissolution behavior of residual NAPL have generally neglected wettability considerations. These approaches include the development of mass transfer correlations [*Miller et al*., 1990; *Parker et al*., 1991; *Powers et al*., 1994a; *Imhoff et al*., 1994, 1997] and attempts to explicitly model temporal changes in the interfacial area during dissolution [*Geller and Hunt*, 1993; *Powers et al*., 1994b]. It should be mentioned that more complicated mathematical expressions that divide the domain into regions in which different mechanisms (e.g., equilibrium and rate-limited) are controlling [e.g., *Rixey*, 1996; *Garg and Rixey*, 1999], have been developed to describe rate-limited dissolution behavior. The research described herein was undertaken to explore the influence of fractional wettability on the long-term dissolution of an entrapped NAPL. A series of column experiments was conducted for dissolution of tetrachloroethylene entrapped in porous media representing a range of grain sizes, gradations, and fractional wettabilities. An understanding of the influence of wettability variations on the entrapment of residual NAPL and its subsequent dissolution should facilitate the prediction of NAPL persistence in natural soils.

2. Materials and Methods

This section outlines the media, fluids, and experimental procedures that were employed in this investigation. The experimental porous media consisted of various sieve sizes of Ottawa sands as indicated in Table 1. Here, the median grain size (d_{50}, in centimeters) and the uniformity index ($U_i = d_{60}/d_{10}$) are measures of the average grain size and the distribution of grain sizes, respectively; here $x\%$ of the mass is finer than d_x. Some of the sands were treated with a 3–5% solution (by volume) of octadecyltrichlorosilane (OTS) in ethanol to render them hydrophobic according to the procedure presented by *Anderson et al*. [1991]. The receding and advancing tetrachloroethylene (PCE)–water contact angles of OTS-treated quartz slides were measured as 148° and 169°, respectively. Fractional wettability media were obtained by mixing various mass fractions of untreated and OTS-treated Ottawa sands. The final column in Table 1 presents the matrix of fractional wettability media that were employed in the dissolution experiments described herein.

The fluids employed in the experiments were Milli-Q water, and laboratory grade (99%) PCE (Aldrich Chemical Co., Milwaukee, Wisconsin). PCE has a density ρ_0 of 1.623 g/cm^3, a viscosity μ_0 of 0.89 cP [*Lide*, 1994], and an interfacial tension σ_{0w} of 45.0 dyn/cm [*Brown et al*., 1994]. The equilibrium solubility C_s of PCE was determined from batch experiments to be approximately 203 mg/L at 20°C. This value compares favorably with the value of 200 mg/L previously reported by *Gillham and Rao* [1990]. An estimated value for the aqueous phase diffusion coefficient D_0 of PCE is 6.57×10^{-6} cm^2/s at this temperature [*Hayduk and Laudie*, 1974].

Custom-designed aluminum columns, 4.8 cm long and 5 cm ID, were dry packed with the various fractional wettability media. Care was taken to ensure a uniform packing by completely mixing small quantities of the appropriate sieve size and wettability fractions before addition to the columns. After each incremental addition of soil, a wooden plunger was placed on top of the sand and the columns were briefly vibrated to minimize any settling and layering. These columns were then flushed with several pore volumes (PV, the product of the porosity and column volume) of carbon dioxide, followed by approximately 200 PV of Milli-Q water to saturate them. Table 2 provides porosity (ε) values for each experimental soil column. The porosity was determined according to the method of *Danielson and Sutherland* [1986] using the measured soil bulk density and assuming a specific solid density of 2.65 g/cm^3.

Figure 1 is a schematic of the experimental setup employed for PCE entrapment. Water- and NAPL-wet ceramic plates (1 or 0.5 bar) were placed on the top and bottom of the column, respectively. Residual water saturation was attained by displacing water from the column with PCE by incrementally adjusting the boundary conditions for water and PCE reservoirs, which were hydraulically connected to the columns via the capillary barriers (ceramics). The maximum capillary pressure (water pressure minus PCE pressure) enforced across the columns ranged from 150 to 300 cm of water, depending on the soil type and wettability characteristics. The maximum capillary pressure was imposed for ~12 hours, until flow had visibly ceased. Boundary pressures were selected to ensure that more than 70% of the pore space was filled with PCE. A residual PCE saturation was similarly attained by displacing PCE from the column with water by incrementally adjusting the boundary pressure conditions. In this case, a minimum capillary pressure was enforced across the columns ranging from −150 to −300 cm of water.

To confirm the uniformity of PCE entrapment and to explore the spatial distribution of residual NAPL, some of the columns were scanned with a computer-aided-tomography X-

Table 2. Physical Properties of Experimental Systems

Soil	OTS%	Porosity ε	Residual Volumetric Content θ_{r0}	Residual Saturation S_{r0}	Darcy Velocity q, cm/min
F20-F30	0	0.327	0.0419	0.1284	0.516
	10	0.318	0.0173	0.0546	0.466
	25	0.324	0.0184	0.0567	0.481
	50	0.337	0.0198	0.0587	0.503
	75	0.342	0.0089	0.0260	0.512
F35-F50	0	0.321	0.0357	0.1112	0.451
	10	0.314	0.0307	0.0979	0.480
	25	0.341	0.0209	0.0614	0.471
(Replicate)	25	0.314	0.0245	0.0779	0.539
	50	0.341	0.0242	0.0711	0.487
	75	0.325	0.0173	0.0534	0.551
	100	0.341	0.0210	0.0616	0.470
F70-F110	0	0.316	0.0451	0.1430	0.549
	10	0.326	0.0487	0.1495	0.493
	25	0.342	0.0299	0.0872	0.481
	50	0.340	0.0344	0.1012	0.455
	75	0.346	0.0326	0.0934	0.481
	100	0.348	0.0853	0.2454	0.479
F35-F50-F70-F110	0	0.302	0.0344	0.11386	0.480
	10	0.301	0.0399	0.13240	0.497
	25	0.294	0.0217	0.07374	0.500
	50	0.298	0.0149	0.04999	0.520
	75	0.313	0.0301	0.09610	0.499
	100	0.306	0.0361	0.11803	0.509

ray (CAT scan) system. The General Electric CT 9800 CAT scan system was operated for 4-s intervals at a current setting of 140 mA and a voltage setting of 80 kVp. The high-resolution setting of this machine was employed to obtain CAT scan numbers for various locations in the columns at a scale of 0.5 mm × 0.5 mm × 1.5 mm. Residual PCE saturations were subsequently obtained using the procedure outlined by *Vinegar and Wellington* [1986]. The CAT scans confirmed that reasonably uniform residual PCE distributions were achieved along the columns using the entrapment protocol. The resolution of these CAT scan images, however, was insufficient to visualize the pore-scale distribution of residual PCE films and ganglia. Use of the CAT scan technique was not pursued further because of this limitation.

Following entrapment, PCE dissolution experiments were conducted in the columns. Figure 1 presents the experimental setup employed in these dissolution experiments. Milli-Q water was pumped upward through the columns at a steady rate with a Masterflex L/S 10-channel drive pump. The average aqueous Darcy velocity q for the various soil columns is given in Table 2. Aqueous phase samples (0.1 mL) were periodically collected in duplicate from the effluent stream from a syringe port and then injected into sealed 1.5-mL Wheaton autosampler vials containing 1 mL of hexane. The vials were subsequently shaken to insure complete extraction of PCE from the

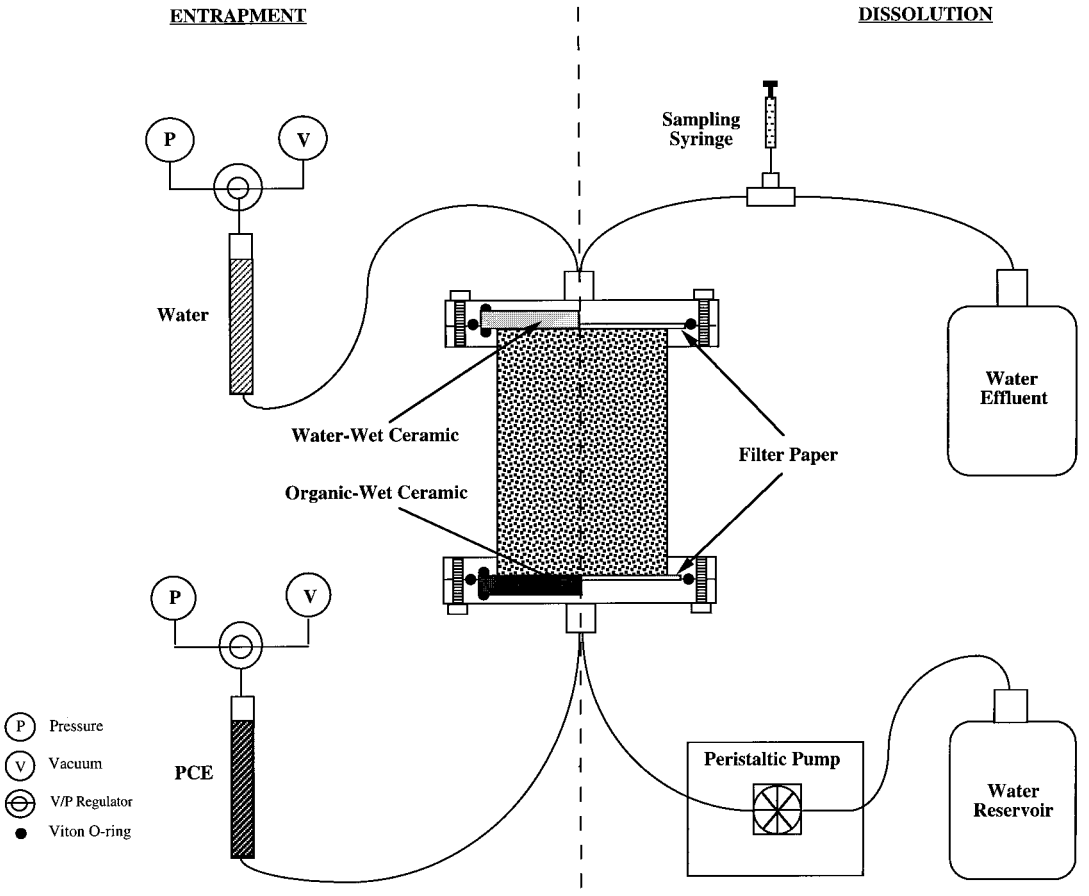

Figure 1. Schematic of the experimental setup employed for PCE entrapment and dissolution.

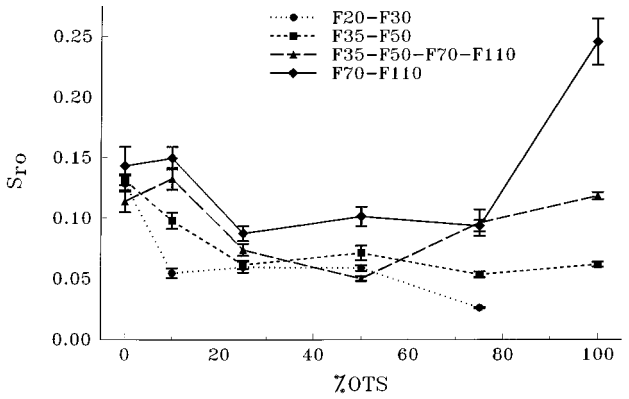

Figure 2. Residual PCE saturation (S_{r0}) versus the organosilane-treated soil mass fraction (OTS%) for the indicated sieve sizes of Ottawa sands.

aqueous samples by hexane. Concentrations were then analyzed with a Hewlett-Packard 5890 gas chromatograph (GC) equipped with an electron capture detector (ECD). The detection limit for this GC/extraction technique was approximately 0.051 mg/L or a relative (C_s = 203 mg/L) effluent concentration of 2.5×10^{-4}. Effluent concentrations were determined as averages of two injections for each replicate effluent sample at each sampling time. Flushing experiments were continued until the separate phase PCE was "completely" recovered; i.e., effluent concentrations dropped 3–4 orders of magnitude below the equilibrium solubility. Removal of nonaqueous phase PCE was confirmed for several of the columns by monitoring effluent concentrations before and after a flow interruption. Theoretically, if separate phase PCE is still present in a column, the effluent concentration should rebound to near equilibrium solubility levels when flow is reinitiated, provided that the flow interruption occurs for a sufficient duration [*Pennell et al*., 1993].

The cumulative PCE volumetric content θ_0 recovered in the aqueous phase at time t was calculated from

$$\theta_0(t) = \frac{Q}{\rho_0 V_T} \int_0^t C(t^*)\, dt^* \qquad (1)$$

where Q is the aqueous phase flow rate (liters per minute), V_T is the total column volume (cubic centimeters), t^* is a dummy time variable (minutes), and C is the concentration (milligrams per liter) (mg/L) of PCE in the aqueous phase. The initial residual PCE volumetric content entrapped in the columns, θ_{r0}, was estimated by setting t equal to the ending time of the experiment. Independent estimates of the residual saturation obtained from other mass balance considerations are believed to be considerably less accurate than (1) owing to the experimental protocol, which required changing end plates between the entrapment and dissolution portions of the experiments.

3. Experimental Results and Discussion

3.1. Entrapment

The magnitude of the residual NAPL saturation S_{r0} has been reported to depend on experimental emplacement protocols [*Morrow et al*., 1988] and the NAPL continuity, which is a function of pore structure and the spatial distribution of NAPL-wet solids [*Morrow and Mungan*, 1971; *Lorenz et al*., 1974; *Morrow*, 1976]. In water-wet systems, *Morrow et al*. [1988] found that residual nonwetting phase entrapment was dependent on the magnitude of the capillary ($N_C = \mu_w q/\sigma_{0w}$; where μ_w and q are the aqueous phase viscosity and Darcy velocity, respectively) and bond ($N_B = (\rho_0 - \rho_w)gr^2/\sigma_{0w}$, where ρ_w is the aqueous phase density, g is the acceleration due to gravity, and r is the mean soil grain size radius equal to $d_{50}/2$) numbers. For the experimental systems employed in this study, N_C never exceeded 2×10^{-6}, and N_B ranged from 7.3×10^{-4} to 1.6×10^{-2}. *Morrow et al*. [1988] concluded that variations in N_C and N_B of this magnitude could at most account for variations of 1.4–15.5% in the magnitude of the entrapped NAPL saturation in a particular medium. Unfortunately, their analysis is strictly valid for water-wet systems, and no systematic studies have been conducted to explore the coupled influence of experimental emplacement protocols (N_C and N_B) and wettability on NAPL entrapment. To interpret the residual saturation data presented below, it is assumed that S_{r0} variability can be attributed primarily to soil texture and wettability characteristics, and not to the experimental emplacement protocols.

Estimated values of entrapped PCE volumetric content (θ_{r0}) and residual saturation ($S_{r0} = \theta_{r0}/\varepsilon$) for each of the column experiments are presented in Table 2. Figure 2 presents these S_{r0} values as function of the NAPL-wet mass fraction (OTS%) for each of the sands (see Table 1). The 95% confidence intervals reported in the figure are based upon the variability in measured effluent concentrations (analytic error) for the individual columns. It should be noted that these confidence intervals do not reflect the potential variability in residual saturations due to differences in column packing (e.g., microscopic differences in soil grain size distribution); sufficient replicate experiments were not available to quantify such uncertainty. Despite the scatter in S_{r0} values, the plotted data suggest that wettability variations can have a strong influence on residual NAPL entrapment. Here the magnitude of residual saturations for the sands varies as much as 52 to 80% as wettability is altered. A number of studies in the petroleum literature [see *Morrow and Mungan*, 1971; *Lorenz et al*., 1974; *Morrow*, 1976, 1990] have reported a similar influence of wettability on entrapped NAPL residuals in sandstone and in glass micromodels during waterflooding. The value of S_{r0} in sandstone cores has typically been found to be lowest under neutral wettability conditions [*Lorenz et al*., 1974]. Observe in Figure 2 that the residual NAPL saturation in finer-textured (F35-F50-F70-F110 and F70-F110) soils follows a similar pattern, reaching a minimum at intermediate OTS percentages. In contrast, the residual NAPL saturation of coarser-textured (F20-F30 and F35-F50) soils tends to decrease and plateau with increasing OTS percentages. One possible explanation for these observations is that the presence of NAPL films facilitates the drainage and/or depletion of ganglia, which otherwise are entrapped near water-wet solids. As the OTS percentage increases, more NAPL is retained as films. In the case of the finer-textured F35-F50-F70-F110 and F70-F110 soils, the relatively high surface area of these soils leads to increasing NAPL saturations with increasing OTS percentages. In contrast, the coarser-textured soils have a relatively low surface area, and hence increases in the OTS percentage do not lead to significant increases in the NAPL saturation.

A second trend that may be observed in Figure 2 is increasing residual NAPL saturation with decreasing mean grain size at a given wettability condition. This trend may be due in part to the reported dependence of the residual saturation on N_B

[*Morrow et al.*, 1988] (N_B increases and S_{r0} deceases with increases in the mean grain size). An inverse correlation of residual saturation with grain size for media with NAPL-wet solids can also be easily explained in terms of the relationship between increasing solid surface area and decreasing permeability [*Carman*, 1937]. Similar trends were also reported for water-wet sands by *Dekker and Abriola* [1999], who presented a correlation for residual NAPL saturation as a function of intrinsic permeability. This correlation was developed from the data of *Powers* [1992] and *Hoag and Marley* [1986].

3.2. Dissolution

Effluent data from a representative dissolution experiment are plotted in Figure 3. Here effluent concentrations represent PCE recovery from the 100% OTS-coated, graded Ottawa sand (F35-F50-F70-F110). In Figure 3 the log of the normalized concentration (C/C_s) is plotted versus number of liters of water flushed through the column. Error bars, for the 95% confidence intervals, based upon replicate measurements, are also presented. If the error bar is not visible, it is smaller than the symbol. Note that effluent concentrations are high for an initial period and then tend to decrease over time (volume) until a low concentration level (tailing) is attained. This decreasing concentration trend can be attributed to changes in NAPL-water interfacial area as the PCE dissolves. Although similar concentration trends were observed in all dissolution experiments, variations in sand texture and wettability conditions created substantial variability in the shapes of the falling portion of the concentration curves.

The concentration rebound present in the tailing region of the effluent curve in Figure 3 is associated with a flow interruption of approximately 169.5 hours. When water flow was resumed, effluent concentrations decreased rapidly to the same level that occurred before the flow was stopped. Flow interruption behavior was similar for all dissolution experiments. Note that in the concentration tailing region, error bars appear larger. This is a consequence of the log scale data presentation and of the limits of the analytical method. Similar analytical error behavior was observed in all experiments. For clarity of presentation, subsequent figures present neither error bars nor flow interrupt data. Table 3, however, summarizes flow interrupt information, which is discussed later.

In order to facilitate comparisons among the long-term column dissolution experiments presented herein, the normalized concentration curves have been "shifted" along the abscissa (shifted volume, V'), so that the area under each curve (from $V' = 0$ to the value of V' at the end of the dissolution experiment) represents recovery of the same volume (mass) of PCE. Here a comparison is made among the shapes of effluent concentration curves during the dissolution of the final 0.02 volumetric PCE content in the columns. Since all columns have the same dimension, this dissolved volume is equivalent to 3.185 g of PCE.

Figure 4a presents a semi-log plot of normalized effluent concentrations versus shifted volumes (V') of water flushed through the columns containing F35-F50 sands under different wettability conditions. Note that differences in a medium's wettability characteristics can have a dramatic influence on PCE recovery. In general, an increase in the extent of fractional wettability significantly reduces the flushing volume required to achieve concentrations three orders of magnitude lower than the equilibrium solubility. For columns with lower NAPL-wet fractions (OTS $\leq$ 25%), the influence of the addition of NAPL-wet solids is particularly marked. An increase in NAPL-wet fraction is associated with a longer period of high effluent concentrations, followed by a more rapid decrease in concentration levels to a tailing region. For higher NAPL-wet systems (OTS $\geq$ 50%) there is less sensitivity to an increase in NAPL-wet fraction. Curves for OTS equal to 50, 75, and 100% are remarkably similar, differing primarily in the concentration tailing region.

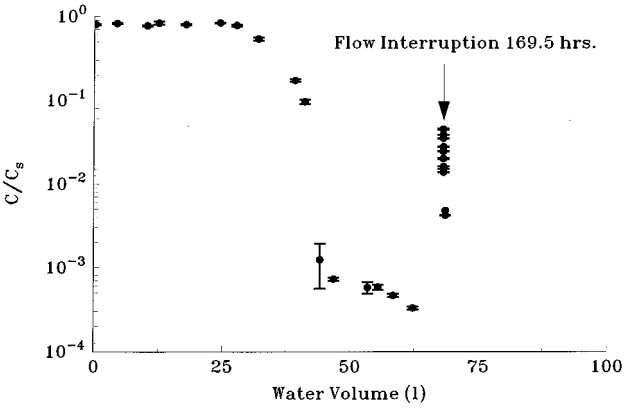

Figure 3. Semilog plot of normalized effluent concentrations (C/C_s) versus pore volumes for an example dissolution data set (100% OTS F35-F50-F70-F110 sand).

Effluent concentration data for other sand size fractions are presented in Figures 4b through 4d. Here again, the influence of an increase in NAPL-wet fraction is readily apparent, with increasing fractional wettability associated with reduced dissolution times. A careful comparison of these figures also suggests that grain size distribution influences the system response to changes in fractional wettability conditions. For example, consider Figure 4c, which presents dissolution data for the most graded sand. Here each increase in NAPL-wet fraction is associated with a change in the dissolution rate. This behavior can be contrasted with that exhibited in Figure 4d by systems composed of the finest (F70-F110) sand fraction. Here curves for OTS $\geq$ 25% are relatively indistinguishable.

A possible explanation for the dissolution behavior shown in Figure 4 is obtained by considering hypothetical PCE distributions in fractional wettability media as shown in Figure 5. In fractional wettability media it is likely that the residual PCE is entrapped both as films covering NAPL-wet solids and as larger ganglia near water-wet solids. The relative proportion of PCE entrapped as films and ganglia depends on both the extent of fractional wettability and the grain size distribution parameters. The dissolution behavior of such residual NAPL is known to be sensitive to the NAPL-water interfacial area [e.g., *Powers et al.*, 1994]. The estimation and modeling of temporal changes in interfacial area during dissolution is beyond the scope of this manuscript. Theoretical approaches to estimate NAPL-water interfacial areas, however, suggest that the area to volume ratio of the entrapped NAPL will be much higher when the PCE is distributed as films than when it occurs as ganglia, and that this ratio will increase with increasing NAPL-wet fraction and decreasing mean grain size [*Gvirtzman and Roberts*, 1991; *Bradford and Leij*, 1997]. Consequently, the presence of PCE films is likely responsible for the longer periods of high effluent concentrations in the higher OTS% systems. The existence of films in contact with ganglia may provide a source of replenishment to the films and promote

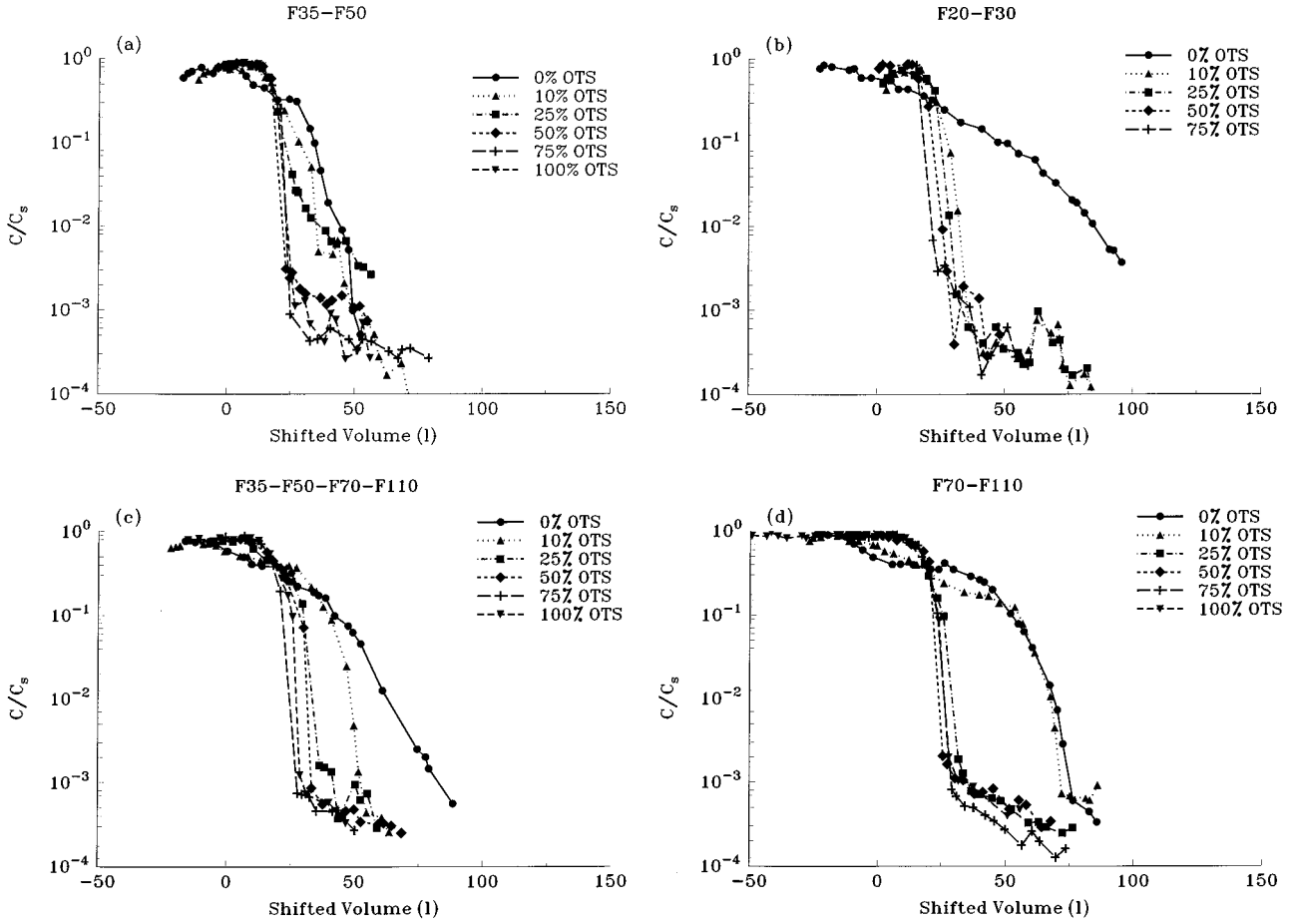

Figure 4. Plot of the log of C/C_s versus shifted volume V' of water flowing through the various soil columns containing (a) F35-F50, (b) F20-F30, (c) F35-F50-F70-F110, and (d) F70-F110 sands.

depletion of the ganglia, which would facilitate the maintenance of high interfacial areas and effluent concentrations during dissolution. Once the PCE films are dissolved, a dramatic decrease in interfacial area is hypothesized to occur, which would lead to a sudden drop-off in concentration.

The dissolution behavior in the high OTS soils is further examined in Figure 6a, which presents effluent concentration data for columns containing 75% OTS media. The NAPL configuration and dissolution behavior of the 50 and 100% OTS media are almost identical to those of the 75% OTS soils and therefore are not presented. Note in Figure 6a that the long-term dissolution behavior for the various grain size distributions is very similar. The initial effluent concentrations are near equilibrium, followed by a dramatic decrease in concentration, and similar low concentration tailing. This behavior can be attributed to the fact that the residual PCE is distributed mainly as NAPL films coating the OTS-treated solid surfaces. The NAPL films have a high interfacial area, which allows high effluent concentrations to be maintained until more than 99% of the mass is removed. The remaining NAPL mass, which is responsible for the tailing behavior at low effluent concentrations, is discussed later in this section.

Mass transfer behavior similar to that shown in Figure 6a has been observed in volatilization studies when the residual NAPL spreads on the residual water-air interface [*Abriola et al*., 1999]. Both systems may have comparable pore-scale configurations of the residual NAPL. In studies of initial entrapped NAPL phase volatilization, *Wilkins et al*. [1995] observed that mass transfer rates were proportional to the mean grain size and independent of the uniformity coefficient. Assuming comparable residual NAPL distributions in the two

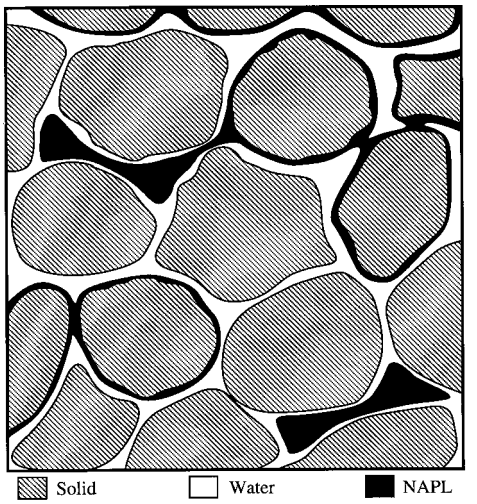

Figure 5. Hypothetical pore-scale distributions of PCE in a fractional wettability porous medium. Reproduced with permission from *Environmental Health Perspectives* [*Abriola and Bradford*, 1998].

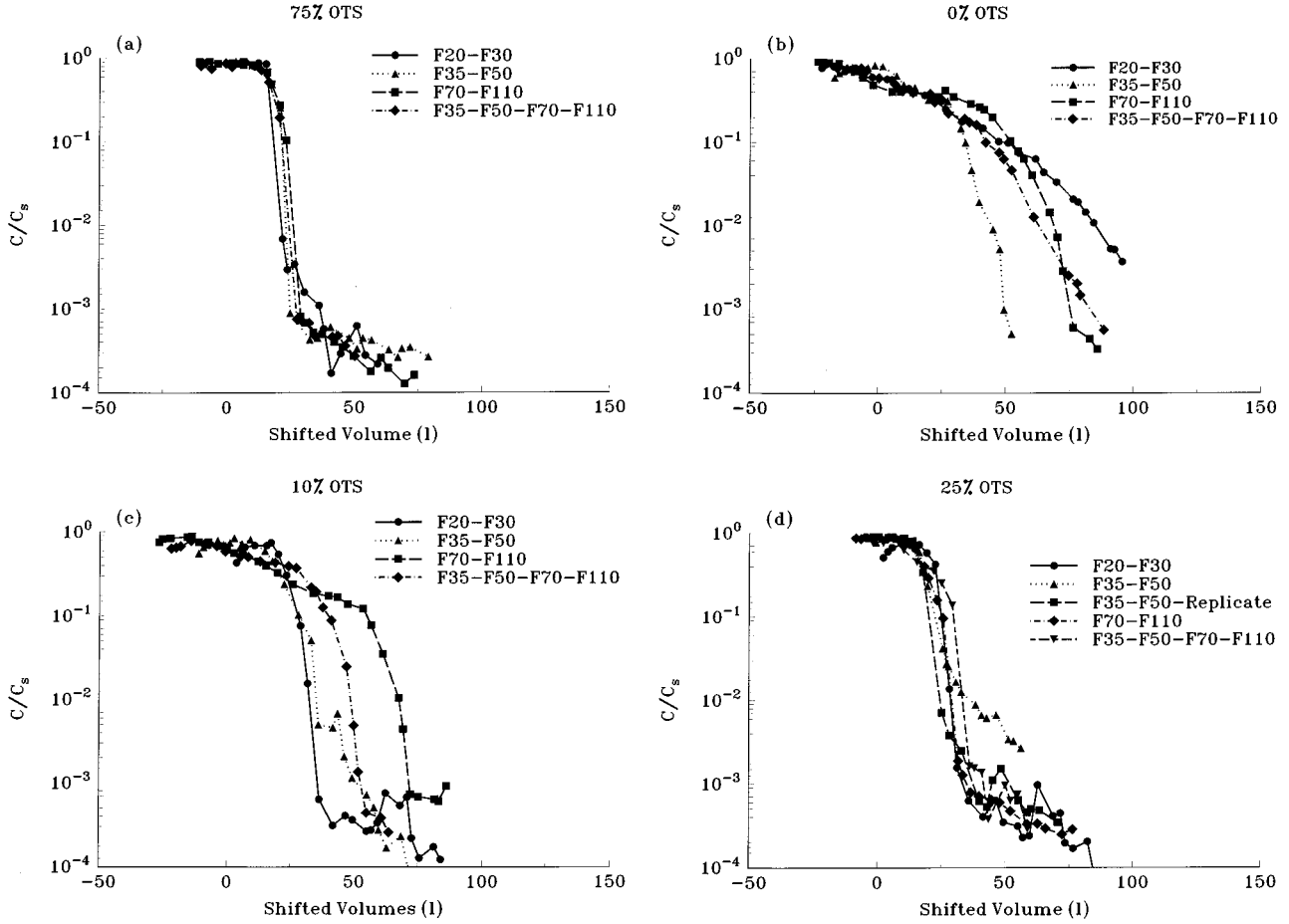

Figure 6. Log plot of C/C_s versus shifted volumes V' of water flowing through the columns containing (a) 75, (b) 0, (c) 10, and (d) 25% OTS media.

systems, this would suggest that faster dissolution times should occur in the coarser-textured soils. Observe in Figure 6a that the coarser-textured soils do exhibit slightly faster dissolution times than the finer-textured materials.

In water-wet media the long-term dissolution behavior has been demonstrated to be associated with the interfacial area of the entrapped ganglia [*Powers et al*., 1994a]. As dissolution proceeds, the interfacial area of the ganglia is hypothesized to slowly decrease as the ganglia decrease in size. Ganglia that possess a lower interfacial area per NAPL volume, as found in coarser and more graded soils, are theoretically most persistent [*Powers et al*., 1992]. Figure 6b presents a plot of effluent concentration for columns containing 0% OTS media. Observe that the various size fractions of Ottawa sand exhibit gradual changes in effluent concentrations over prolonged periods, attributed to the slow dissolution of the entrapped PCE ganglia. The dissolution time was shortest for the F35-F50 sand, followed by the F70-F110 and the F35-F50-F70-F110 sands, and then finally the coarsest F20-F30 sands.

Powers et al. [1994a] reported that dissolution time increases with increasing mean grain size and uniformity coefficient. The dissolution data presented in Figure 6b do not follow this trend. This discrepancy is not fully understood at present but may be due to differences between the soil grain size distributions used in each study. For example, *Powers et al*. [1994a] utilized soils with mean grain sizes ranging from 0.045 to 0.12 cm, whereas this study encompasses sands ranging from 0.015 to 0.071 cm. The coarser-textured F35-F50 and F20-F30 sands exhibit dissolution behavior similar to that reported by *Powers et al*. [1994a] and have d_{50} values (0.036 and 0.071 cm, respectively) that are most comparable to those in their work. In contrast, the finer textured F70-F110 and F35-F50-F70-F110 sands exhibit significantly longer dissolution times than would be anticipated on the basis of *Powers et al*. [1994a]. One possibility is that the entrapped ganglia are less accessible to flowing water in very fine textured soils. A second related hypothesis is that dissolution fingering may have occurred in the finer-textured sands [*Imhoff and Miller*, 1996; *Imhoff et al*., 1996]. Without further information on the evolution of pore-scale saturation distributions, these explanations cannot be confirmed.

Figure 6c presents effluent concentration data for columns containing 10% OTS media. Observe that the long-term dissolution behavior shows a pronounced dependence on the mean grain size; the dissolution time increases as the mean grain size decreases. This result is somewhat surprising, since for the same NAPL-wet mass fraction, the finer-textured soil is expected to have a higher interfacial area and hence enhanced mass transfer. One possible explanation is obtained by postulating interactions between ganglia and films. For example, suppose that the presence of NAPL films, larger ganglia, and diminished capillary forces in coarser-textured soils facilitates the drainage of ganglia in contact with NAPL films. In support of this hypothesis, observe in Figure 2 that the residual NAPL

Table 3. Flow Interruption Data

Soil	OTS%	Interruption, hours	Shifted Volume, L	Concentration, mg/L
F35-F50	0	20.8	61.55	7.56
	10	20.8	72.63	6.17
	25	39.7	59.07	32.24
	50	39.8	57.91	16.42
	75	39.9	41.41	17.61
	100	39.9	58.91	15.65
F35-F50-F70-F110	0	68.0	104.82	19.26
	10	20.8	65.01	5.93
	25	169.3	64.67	14.30
	50	169.3	74.43	15.34
	75	169.4	55.92	10.61
	100	169.5	52.61	9.18

saturation for the coarser sands decreased substantially with a small addition of NAPL-coated material (10% OTS). If this conceptual model is correct, ganglia would not persist in these 10% coarser-textured media, and a greater fraction of the NAPL mass would be present as films, leading to a higher specific interfacial area. Consequently, the coarser-textured soils would exhibit enhanced mass transfer compared with the finer-textured soils. In further support of this hypothesis, observe in Figure 4b the similarities in dissolution behavior for the 10% and 75% F20-F30 OTS sands, indicating enhanced mass transfer at low OTS%. Analogously, note in Figure 4d the similarity between the 0% and 10% OTS curves for the F70-F110 sand, which suggests that a significant portion of the residual NAPL occurs as ganglia in both sands.

Figure 6d presents effluent concentrations for columns containing 25% OTS media. Comparison of Figures 6d and 6a (75% OTS) reveals very similar dissolution behavior when $C/C_s > 0.01$, and striking differences when $C/C_s < 0.01$. When $C/C_s > 0.01$, the dissolution characteristics of the PCE entrapped in 25% OTS media can be explained in an analogous fashion to that discussed above for Figure 6a. Here relatively constant interfacial areas are maintained due to the presence of NAPL films and/or film-ganglia interactions. In contrast to Figure 6a, however, the most graded F35-F50-F70-F110 sand tends to exhibit more gradual changes in concentration (less curvature), resulting in a slightly longer dissolution time. Similar behavior was observed for the 50% OTS F35-F50-F70-F100 soil (see Figure 4). It is hypothesized that this difference in dissolution behavior can be attributed to the presence of less accessible NAPL films. In the more graded F35-F50-F70-F110 soil, NAPL films in the larger pores would tend to dissolve more rapidly than those in finer pores, owing to a decreased residence time for water and hence a larger concentration gradient at the NAPL-water interface in larger pores. The influence of such films would only be apparent after significant removal of the NAPL mass from the more accessible portions of the pore space, and hence calculated initial mass transfer rates would not likely show a strong dependence on the uniformity coefficient.

Note in Figure 6d the dissolution tailing behavior when C/C_s is less than 0.01. The tailing behavior of the F35-F50 and F35-F50-F70-F110 sands, in particular, may occur as a result of isolated lower interfacial area ganglia that do not interact with the NAPL films. Such ganglia would dissolve at a slower rate than NAPL films or ganglia-film combinations and hence would not become apparent until most of the NAPL had dissolved. The presence or absence of such isolated ganglia are likely very sensitive to the pore-scale distribution of NAPL-wet sands in the soil column and hence less reproducible. The observed differences between the tailing behavior in the replicate F35-F50 sand experiments supports this hypothesis.

The persistent concentration tailing behavior observed in Figures 4 and 6 could be attributed to (1) desorption of PCE from the sands, (2) the presence of persistent PCE ganglia, which dissolve more slowly than the PCE films owing to their lower interfacial area per volume ratio, and/or (3) the presence of less accessible PCE films. The possibility that the presence of separate phase PCE was responsible for the observed concentration tailing was investigated by interrupting water flow in some of the experiments. Table 3 summarizes flow interruption data obtained at the end of several soil column dissolution experiments. A precise analysis of these flow interrupt data is complicated by the dependence of the concentration rebound on OTS percentage, flow interruption duration, and volume flushed before the interruption. Observe that for a given flow interruption duration, the concentration rebounds tended to be highest for water-wet and lower OTS percentage soils. If no separate phase PCE were present in the columns, then the opposite trend would be anticipated based upon the sorption capacity of the soils; i.e., higher-OTS soils have the greatest sorption capacity. This observation suggests that limited amounts of separate phase PCE (low interfacial area ganglia) may have been present in some of the low-OTS soils. Note, however, that the concentration rebound was always less than 16% of C_s, suggesting that very little PCE remained. S. A. Bradford et al. (Dissolution of residual tetrachloroethene in fractional wettability porous media: Correlation development and application, submitted to *Journal of Contaminant Hydrology*, 1999) recently analyzed the long-term fractional wettability dissolution data presented herein using numerical modeling and measured equilibrium sorption parameters. Their results suggest that rate-limited desorption can adequately describe the observed low-concentration tailing behavior of the higher OTS fraction soils. *Imhoff et al*. [1998] also reported that rate-limited desorption was responsible for the low concentration tailing observed in their long-term dissolution data.

4. Summary and Conclusions

This paper presents experimental studies investigating the entrapment and long-term dissolution behavior of residual PCE in sandy porous media, encompassing a wide range of grain size distribution parameters and fractional wettabilities. Results reported herein indicate that both wettability and grain size distribution characteristics are important parameters in determining the entrapment and the long-term dissolution behavior of residual NAPLs.

For a given soil wettability, the magnitude of the residual NAPL saturation tended to increase with decreasing mean grain size. In fractional wettability soils this result is likely due to increases in NAPL-wet solid surface area with decreases in the mean grain size. The influence of wettability on the residual NAPL saturation was also found to depend on the soil mean grain size. In finer-textured soils, the residual NAPL saturation tended to achieve a minimum for intermediate OTS percentages. The initial decrease in residual saturation with increasing OTS percentage was attributed to the depletion and/or drainage of ganglia near water-wet sands by NAPL films. Further increases in the OTS percentage led to increases

in the residual NAPL saturation, presumably due to increasing coverage of the relatively high surface area OTS sand fraction. In coarser-textured sands, however, the residual NAPL saturation tended to decrease and plateau with increasing OTS percentages. This observation was again attributed to the depletion and/or drainage of ganglia by NAPL films. Here, however, diminished capillary forces and increasing ganglia size were hypothesized to facilitate the drainage of the ganglia. The relatively low surface area of these coarser sands was also hypothesized to be responsible for the diminished sensitivity of the residual saturation to further increases in the OTS percentage.

Previous dissolution studies and mass transfer correlations have neglected wettability considerations. The experimental studies reported herein demonstrate that fractional wettability significantly influences the long-term dissolution behavior of residual PCE. Effluent concentration curves for the water-wet media exhibited gradual concentration changes over time (volume), attributed to the presence of low interfacial area ganglia which dissolve slowly. In contrast, fractional wettability systems achieved effluent concentrations 3 orders of magnitude below the equilibrium solubility much more rapidly. This result was attributed to the presence of higher interfacial area PCE films coating the OTS treated sands. For a given soil grain size distribution, increases in the OTS mass fraction led to an increase in the NAPL-water interfacial area and hence a decrease in the dissolution time. Benefits derived from this reduced dissolution time may be partially offset by the increased sorption capacity of fractional wettability soils, which was hypothesized to be responsible for the observed rate-limited low level concentration tailing ($C/C_s < 10^{-3}$).

Results also indicate that the influence of fractional wettability on the long-term dissolution behavior of PCE is strongly dependent on the soil grain size distribution characteristics. The effects of grain size distribution parameters were especially pronounced for soils consisting of low OTS percentages. For coarse-grained media a dramatic decrease in the dissolution time was observed when a small proportion of NAPL-wet grains (10%) was present. This behavior was attributed to alteration of the residual NAPL saturation configuration due to ganglia drainage by film flow. The dissolution behavior of PCE in soils composed of 25 and 50% OTS percentages was also observed to be sensitive to changes in soil gradation. For these systems the NAPL was hypothesized to occur primarily as NAPL films, with a few isolated ganglia that are strongly dependent on the pore-scale distribution of OTS sands. Variable accessibility of the NAPL films to flowing water, as a result of soil gradation in these systems, was hypothesized to be responsible for the observed increase in dissolution time for the most graded soil.

There is currently little available information on subsurface variations in soil wetting properties. Results presented herein indicate that wettability characteristics should be considered in NAPL entrapment and dissolution studies. Hence there is presently a need to quantify wettability parameters in natural soils and subsurface formations. Future research will investigate the entrapment and dissolution of NAPLs in natural soils, and the application of these findings to larger-scale aquifer environments.

Acknowledgments. Funding for this research was provided by the National Institute of Environmental Health Sciences under grant ES04911. The research described in this article has not been subject to agency review and therefore does not necessarily reflect the views of the agency, and no official endorsement should be inferred.

References

Abriola, L. M., and S. A. Bradford, Experimental investigations of the entrapment and persistence of organic liquid contaminants in the subsurface environment, *Environ. Health Perspect*., *106*, 1083–1095, 1998.

Abriola, L. M., K. D. Pennell, W. J. Weber Jr., J. R. Lang, and M. D. Wilkins, Persistence and interphase mass transfer of organic contaminants in the unsaturated zone: Experimental observations and mathematical modeling, in *Vadose Zone Hydrology: Cutting Across Disciplines*, edited by J. Y. Parlange and J. W. Hopmans, Oxford Univ. Press, New York, in press, 1999.

Anderson, R., G. Larson, and C. Smith, *Silicon Compounds: Register and Review*, 5th ed., Huls America Inc., Piscataway, N. J., 1991.

Anderson, W. G., Wettability literature survey, 1, Rock/oil/brine interactions and the effects of core handling on wettability, *J. Pet. Technol*., *38*, 1125–1144, 1986.

Bradford, S. A., and F. J. Leij, Estimating interfacial areas for multifluid soil systems, *J. Contam. Hydrol*., *27*, 83–105, 1997.

Brown, C. L., G. A. Pope, L. M. Abriola, and K. Sepehrnoori, Simulation of surfactant-enhanced aquifer remediation, *Water Resour. Res*., *30*, 2959–2977, 1994.

Brown, R. J. S., and I. Fatt, Measurements of fractional wettability of oilfield rocks by the nuclear magnetic relaxation method, *Trans. Am. Inst. Min. Metall. Pet. Eng*., *207*, 262–264, 1956.

Carman, P. C., Fluid flow through a granular bed, *Trans. Inst. Chem. Eng*., *23*, 150–156, 1937.

Chatzis, I., N. R. Morrow, and H. T. Lim, Magnitude and detailed structure of residual oil saturation, *Soc. Pet. Eng. J*., *23*, 311–326, 1983.

Danielson, R. E., and P. L. Sutherland, Porosity, in *Methods Soil Analysis*, Part 1, *Physical and Mineralogical Methods*, 2nd ed., edited by A. Klute, Soil Sci. Soc. Am., Madison, Wis., 1986.

Dekker, L. W., and C. J. Ritsema, How water moves in a water repellent sandy soil, 1, Potential and actual water repellency, *Water Resour. Res*., *30*, 2507–2519, 1994.

Dekker, T. J., and L. M. Abriola, The influence of field-scale heterogeneity on the infiltration and entrapment of dense nonaqueous phase liquids in saturated formations, *J. Contam. Hydrol*., in press, 1999.

Demond, A. H., F. N. Desai, and K. F. Hayes, Effect of cationic surfactants on organic liquid-water capillary pressure-saturation relationships, *Water Resour. Res*., *30*, 333–342, 1994.

Donaldson, E. C., R. D. Thomas, and P. B. Lorenz, Wettability determination and its effect on recovery efficiency, *Soc. Pet. Eng. J*., *9*, 13–20, 1969.

Dragun, J., A. C. Kuffner, and R. W. Schneiter, Groundwater contamination, I, Transport and transformations of organic chemicals, *Chem. Eng*., *91*, 65–70, 1984.

Garg, S., and W. G. Rixey, The dissolution of benzene, toluene, m-xylene and naphthalene from a residually trapped non-aqueous phase liquid under mass transfer limited conditions, *J. Contam. Hydrol*., *36*, 313–331, 1999.

Geller, J. T., and J. R. Hunt, Mass transfer from nonaqueous phase organic liquids in water-saturated porous media, *Water Resour. Res*., *29*, 833–846, 1993.

Gillham, R. W., and P. S. C. Rao, Transport, distribution, and fate of volatile organic compounds in groundwater, in *Significance and Treatment of Volatile Organic Compounds in Water Supplies*, edited by N. M. Ram, F. C. Russel, and K. P. Contor, pp. 141–181, Lewis, Boca Raton, Fla., 1990.

Guarnaccia, J. F., P. T. Imhoff, B. C. Missildine, M. Oostrom, M. A. Celia, J. H. Dane, P. R. Jaffe, and G. F. Pinder, Multiphase chemical transport in porous media, final report, *EPA/600/S-92/002*, U.S. Environ. Prot. Agency, Washington, D. C., 1992.

Gvirtzman, H., and P. V. Roberts, Pore scale spatial analysis of two immiscible fluids in porous media, *Water Resour. Res*., *27*, 1165–1176, 1991.

Hayduk, W., and H. Laudie, Prediction of diffusion coefficients for nonelectrolytes in dilute aqueous solutions, *AIChE J*., *20*, 611–615, 1974.

Hoag, G. E., and M. C. Marley, Gasoline residual saturation in unsat-

urated uniform aquifer materials, *J. Environ. Eng*., *112*, 586–604, 1986.

Hunt, J. R., N. Sitar, and K. S. Udell, Nonaqueous phase liquid transport and cleanup, 1, Analysis of mechanisms, *Water Resour. Res*., *24*, 1247–1258, 1988.

Imhoff, P. T., and C. T. Miller, Dissolution fingering during the solubilization of nonaqueous phase liquids in saturated porous media, 1, Model predictions, *Water Resour. Res*., *32*, 1919–1928, 1996.

Imhoff, P. T., P. R. Jaffe, and G. F. Pinder, An experimental study of complete dissolution of a nonaqueous phase liquid in a saturated porous media, *Water Resour. Res*., *30*, 307–320, 1994.

Imhoff, P. T., G. P. Thyrum, and C. T. Miller, Dissolution fingering during the solubilization of nonaqueous phase liquids in saturated porous media, 2, Experimental observations, *Water Resour. Res*., *32*, 1929–1942, 1996.

Imhoff, P. T., A. Frizzell, and C. T. Miller, Evaluation of thermal effects on the dissolution of a nonaqueous phase liquid in porous media, *Environ. Sci. Technol*., *31*, 1615–1622, 1997.

Imhoff, P. T., M. H. Arthur, and C. T. Miller, Complete dissolution of trichloroethylene in saturated porous media, *Environ. Sci. Technol*., *32*, 2417–2424, 1998.

Kavanaugh, M. C., Contaminant site remediation—Technology versus public policy, *Water Environ. Res*., *68*, 963–964, 1996.

Land, C. S., Calculation of imbibition relative permeability for two- and three-phase flow from rock properties, *Soc. Pet. Eng. J*., *8*, 149–156, 1968.

Lide, D. R., *CRC Handbook of Chemistry and Physics*, 5th ed., CRC Press, Boca Raton, Fla., 1994.

Lorenz, P. B., E. C. Donaldson, and R. D. Thomas, Use of centrifugal measurements of wettability to predict oil recovery, *Rep. 7873*, Energy Technology Center, U.S. Bur. of Mines, Bartlesville, Okla., 1974.

Mayer, A. S., and C. T. Miller, The influences of porous medium characteristics and measurement scale on pore-scale distributions of residual nonaqueous phase liquids, *J. Contam. Hydrol*., *11*, 189–213, 1992.

Miller, C. T., M. M. Poirier-McNeill, and A. S. Mayer, Dissolution of trapped nonaqueous phase liquids: Mass transfer characteristics, *Water Resour. Res*., *26*, 2783–2796, 1990.

Morrow, N. R., The effects of surface roughness on contact angle with special reference to petroleum recovery, *J. Can. Pet. Technol*., *14*, 42–53, 1975.

Morrow, N. R., Capillary pressure correlations for uniformly wetted porous media, *J. Can. Pet. Technol*., *15*, 49–69, 1976.

Morrow, N. R., Wettability and its effect on oil recovery, *J. Pet. Technol*., *42*, 1476–1484, 1990.

Morrow, N. R., and N. Mungan, Wettability and capillarity in porous media, *Rep. RR-7*, Pet. Reservoir Res. Inst., Calgary, Alta., Canada, Jan. 1971.

Morrow, N. R., I. Chatzis, and J. J. Taber, Entrapment and mobilization of residual oil in bead packs, *SPE Reservoir Eng*., *4*, 927–934, 1988.

Parker, J. C., A. K. Katyal, J. J. Kaluarachchi, R. J. Lenhard, T. J. Johnson, K. Jayaraman, K. Jayaraman, K. Unlu, and J. L. Zhu, Modeling multiphase organic chemical transport in soils and ground water, final report, *EPA/600/2-91/042*, U.S. Environ. Prot. Agency, Washington, D. C., 1991.

Pennell, K. D., L. M. Abriola, and W. J. Weber Jr., Surfactant-enhanced solubilization of residual dodecane in soil columns, 1, Experimental investigations, *Environ. Sci. Technol*., *27*, 2332–2340, 1993.

Pfannkuch, H. O., Ground-water contamination by crude oil at the Bemidji, Minnesota, research site: U.S. Geological Survey Toxic Waste–Ground-Water Contamination Study, paper presented at the Toxic Waste Technical Meeting, U.S. Geol. Surv., Reston, Va., 1984.

Powers, S. E., Dissolution of nonaqueous phase liquids in saturated subsurface systems, doctoral thesis, Univ. of Mich., 1992.

Powers, S. E., and M. E. Tamblin, Wettability of porous media after exposure to synthetic gasolines, *J. Contam. Hydrol*., *19*, 105–125, 1995.

Powers, S. E., L. M. Abriola, and W. J. Weber Jr., An experimental investigation of NAPL dissolution in saturated subsurface systems: Steady state mass transfer rates, *Water Resour. Res*., *28*, 2691–2705, 1992.

Powers, S. E., L. M. Abriola, and W. J. Weber Jr., An experimental investigation of NAPL dissolution in saturated subsurface systems: Transient mass transfer rates, *Water Resour. Res*., *30*, 321–332, 1994a.

Powers, S. E., L. M. Abriola, J. S. Dunkin, and W. J. Weber, Jr., Phenomenological models for transient NAPL-water mass-transfer processes, *J. Contam. Hydrol*., *16*, 1–33, 1994b.

Rixey, W. G., The long-term dissolution characteristics of a residually trapped BTX mixture in soil, *Hazardous Waste Hazardous Mater*., *13*, 197–211, 1996.

Salathiel, R. A., Oil recovery by surface film drainage in mixed wettability rocks, *J. Petro. Technol*., *25*, 1216–1224, 1973.

Vinegar, H. J., and S. L. Wellington, Tomographic imaging of three-phase flow experiments, *Rev. Sci. Instrum*., *58*, 96–107, 1986.

Wang, F. H. L., Effect of wettability alteration on water/oil relative permeability, dispersion, and flowable saturation in porous media, *SPE Reservoir Eng*., *4*, 617–628, 1988.

Wilkins, M. D., L. M. Abriola, and K. D. Pennell, An experimental investigation of rate-limited NAPL volatilization in unsaturated porous media: Steady state mass transfer, *Water Resour. Res*., *31*, 2159–2172, 1995.

Wilson, J. L., S. H. Conrad, W. R. Mason, W. Peplinski, and E. Hagan, Laboratory investigation of residual liquid organics from spills, leaks and the disposal of hazardous wastes in groundwater, final report, *EPA/600/6-90/004*, U. S. Environ. Prot. Agency, Washington, D. C., 1990.

L. M. Abriola, S. A. Bradford (corresponding author), and R. A. Vendlinski, Department of Civil and Environmental Engineering, University of Michigan, 181 EWRE, 1351 Beal Avenue, Ann Arbor, MI 48109-2125. (sbrad@engin.umich.edu)

(Received October 22, 1998; revised May 11, 1999;
accepted June 2, 1999.)